Flow aeroacoustic damping using coupled mechanical–electrical impedance in lined pipeline*

Chen Yong(陈 勇)[a)†], Huang Yi-Yong(黄奕勇)[a)], Chen Xiao-Qian(陈小前)[a)], Bai Yu-Zhu(白玉铸)[b)], and Tan Xiao-Dong(谭晓栋)[b)]

[a)] College of Aerospace Science and Engineering, National University of Defense Technology, Changsha 410073, China
[b)] Department of Electronic Technology, Officer's College of CAPF, Chengdu 610213, China

(Received 12 August 2014; revised manuscript received 24 November 2014; published online 27 March 2015)

We report a new noise-damping concept which utilizes a coupled mechanical–electrical acoustic impedance to attenuate an aeroacoustic wave propagating in a moving gas confined by a cylindrical pipeline. An electrical damper is incorporated to the mechanical impedance, either through the piezoelectric, electrostatic, or electro-magnetic principles. Our numerical study shows the advantage of the proposed methodology on wave attenuation. With the development of the micro-electro-mechanical system and material engineering, the proposed configuration may be promising for noise reduction.

Keywords: aeroacoustics, mechanical–electrical impedance, wave propagation, uniform flow

PACS: 43.28.Bj, 43.28.Py, 43.50.Nm **DOI:** 10.1088/1674-1056/24/5/054302

1. Introduction

Reducing noises and emissions in gas flow is of great importance in many industrial applications, especially in aircraft engineering[1] and automotive transport engineering.[2] A typical strategy is to use acoustic lining resonators,[3] among which the Helmholtz resonator[4] may be the widely-used prototype, to absorb noises in gas flow.[5] The physical insight of such methodology is to adjust the boundary conditions of the acoustic wave by configuring the mechanical properties of the resonators.[6]

In the research of energy scavenging for low-power autonomous electronic devices,[7–10] the mechanical vibration, as an attractive energy source due to its high availability in environments, has become an attractive target for energy harvesting.[11–13] Physically, vibration energies can be converted into electronic power with high efficiency through piezoelectric effect,[14–16] electromagnetic effect,[17–19] and electrostatic (coupled with triboelectric) effect.[20–22]

If the energy-harvesting configuration is introduced to noise reduction[23] in gas flow, then the acoustic energy can be partly transformed to electrical energy, which may be dissipated through an electrical circuit loop. More importantly, while only the mechanical properties of the acoustic resonator can be adjusted in the traditional liner configuration, the coupled mechanical–electrical concept adds the freedom of electrical configuration. In the literature, some electroacoustic absorbers were provided to attenuate noises in a stationary gas, which can be found in the studies of Lissek *et al.*,[24] Chang *et al.*,[25] Betgen and Galland,[26] and Liu *et al.*[27]

In this paper, we introduce an electrical damper to the traditional Helmholtz resonator and investigate the performance of noise attenuation in the presence of a uniform mean flow. In what follows, mathematical formulation of the proposed method is comprehensively deduced and the corresponding efficiency of acoustic energy dissipation is investigated by numerically calculating the attenuation coefficient. It should be noticed that the present paper almost concentrates on the theoretical analysis of damping performance while the corresponding fabrication is not provided.

2. Mathematical formulation

The acoustic wave is restricted to propagate along a straight cylindrical duct carrying a perfect gas,[28] while the energy dissipation due to the thermoviscous effect[29] is neglected. The mean flow is purely uniform with zero swirls, while the mean density and the pressure of the flow are constant. To obtain a normalized expression, the radial length is non-dimensionalized through the pipeline radius d_0, and the density is normalized to the mean density ρ_0. Through the uniform sound speed c_0, the flow profile is normalized to the Mach number M.

2.1. Governing equation of wave propagation

If the unsteady perturbations to the mean flow are assumed to be axisymmetric and harmonic, then the unsteady disturbance to the pressure can be written in the form $p' = \varphi_p(r)\exp[\mathrm{i}(\omega t - k_0 K z)]$, where r and z are the radial and axial cylindrical coordinates, respectively, and ω and $k_0 = \omega/c_0$ are

*Project supported by the National Natural Science Foundation of China (Grant Nos. 11404405, 91216201, 51205403, and 11302253).
†Corresponding author. E-mail: literature.chen@gmail.com
© 2015 Chinese Physical Society and IOP Publishing Ltd

the angular acoustic frequency and the inviscid wavenumber, respectively. In this paper, we are interested in the normalized axial wavenumber K because it takes the role of the system's eigenvalue. According to the literature,[30] $\varphi_p(r)$ has an analytical solution expressed as

$$\varphi_p(r) = J_0\left(k_0 d_0 \sqrt{(1-KM)^2 - K^2} r\right). \tag{1}$$

Meanwhile, the radial acoustic velocity can be obtained as

$$v_r' = \frac{\mathrm{i}}{\rho_0 \omega d_0 (1-KM)} \frac{\mathrm{d}\varphi_p}{\mathrm{d}r} \exp[\mathrm{i}(\omega t - k_0 K z)]. \tag{2}$$

2.2. Formulation of the mechanical–electrical impedance

In the literature, the mass–spring–damper model[31] is used to describe the mechanical impedance of a liner, as shown in Fig. 1.

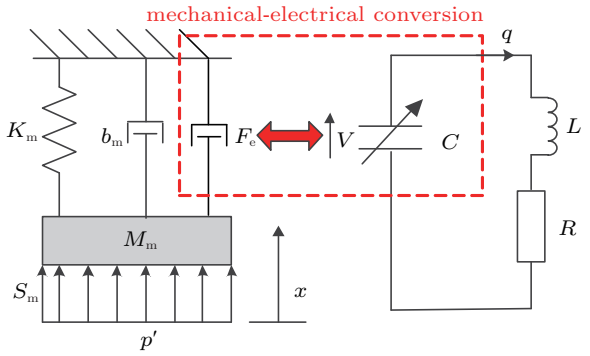


Fig. 1. (color online) The model of the coupled mechanical–electrical impedance resonator. Here S_m denotes the surface area of the resonator.

Specifically, the mass, the spring, and the damping are denoted by M_m, K_m, and b_m, respectively. The electrical damper (denoted by F_e in Fig. 1) can be introduced through either one of the piezoelectric, electromagnetic, and electrostatic (coupled with triboelectric) principles. The produced electric charge q, forced by the converted voltage V, moves through the inductor L, the resistor R, and the capacitor C. Due to the pressure continuity at the fluid-wall interface, the pressure at the wall equals the acoustic pressure p', and excites the particles of the wall to vibrate in the x direction.

By introducing the electromechanical coupling coefficient θ,[13,21] the mechanical and the electrical parts of the acoustic impedance are, respectively, expressed as

$$M_m \frac{\mathrm{d}^2 x}{\mathrm{d}t^2} + b_m \frac{\mathrm{d}x}{\mathrm{d}t} + K_m x - \theta V = S_m p', \tag{3}$$

$$\theta x + VC = -q, \quad V = L\frac{\mathrm{d}^2 q}{\mathrm{d}t^2} + R\frac{\mathrm{d}q}{\mathrm{d}t}$$

$$\Rightarrow \theta L \frac{\mathrm{d}^2 x}{\mathrm{d}t^2} + \theta R \frac{\mathrm{d}x}{\mathrm{d}t} + LC\frac{\mathrm{d}^2 V}{\mathrm{d}t^2} + RC\frac{\mathrm{d}V}{\mathrm{d}t} + V = 0. \tag{4}$$

Due to the harmonic vibration, the voltage V and displacement x are periodically dependent on the time, then equation (4) is simplified to

$$V = \frac{\theta(-L\omega^2 + \mathrm{i}R\omega)}{LC\omega^2 - \mathrm{i}RC\omega - 1} x. \tag{5}$$

Substituting Eq. (5) into Eq. (3) yields

$$-M_m\omega^2 x + \mathrm{i}b_m\omega x + K_m x - \frac{\theta^2(-L\omega^2 + \mathrm{i}R\omega)}{LC\omega^2 - \mathrm{i}RC\omega - 1} x = S_m p'. \tag{6}$$

In the limit of vanishing viscosity, through the continuity of the normal particle displacement[32,33] at the fluid–solid interface, the relationship of the displacement and the acoustic velocity (Eq. (2)) can be written as

$$x = \frac{v_r'}{\mathrm{i}\omega(1-KM)} = \frac{1}{\rho_0 d_0 \omega^2 (1-KM)^2} \frac{\mathrm{d}\varphi_p}{\mathrm{d}x} \exp[\mathrm{i}(\omega t - k_0 K z)]. \tag{7}$$

At the wall ($r = 1$), substituting Eq. (7) into Eq. (6) yields

$$\left[\frac{\mathrm{i}M_m\omega}{S_m} + \frac{b_m}{S_m} + \frac{K_m}{\mathrm{i}\omega S_m} - \frac{\theta^2(R + \mathrm{i}L\omega)}{S_m(LC\omega^2 - \mathrm{i}RC\omega - 1)}\right] \frac{\mathrm{d}\varphi_p}{\mathrm{d}r} = \mathrm{i}\omega\rho_0 d_0 (1-KM)^2 \varphi_p. \tag{8}$$

It should be noticed that the term $Z_m = \mathrm{i}(M_m\omega)/S_m + b_m/S_m + K_m/(\mathrm{i}\omega S_m)$ represents the acoustic mechanical impedance of the wall while the term $Z_e = -\theta^2(R + \mathrm{i}\omega L)/[S_m(LC\omega^2 - \mathrm{i}RC\omega - 1)]$ can be defined as the acoustic electrical impedance. In the absence of electrical damping, the above equation is simplified to the well-established theory.[34]

3. Numerical study

To demonstrate the efficiency of the proposed concept on noise reduction, we consider a configuration of average Mach number $M = 0.1$, mean density $\rho_0 = 1.225$ kg/m^3, adiabatic sound speed $c_0 = 340$ m/s, and pipeline radius $d_0 = 0.03$ m. A Helmholtz type resonator, the impedance of which can be modeled as a mass–spring–damper system near the resonance frequency,[31,34] is fabricated with a cubic cavity (40 mm×40 mm×40 mm) and a narrow neck (28 mm×28 mm×35 mm) anchored into the back plate,[23] the surface area can then be calculated as $S_m = 784$ mm^2. As a result, the acoustic mechanical impedance can be calculated as

$$Z_m = Z_{m0} + \mathrm{i}0.0429\omega - \frac{\mathrm{i}1.74\times 10^6}{\omega}, \tag{9}$$

where the resistance is chosen as $Z_{m0} = 833$ kg/(m^2·s) to be consistent with the literature.[34] In the numerical calculation, the electromechanical coupling θ is assumed to be 1×10^{-2} N/V and the capacitance C is 15 nF.

Figure 2 demonstrates the amplitude and the phase of the acoustic mechanical impedance Z_m and the coupled mechanical–electrical impedance $Z_m + Z_e$ as functions of the acoustic frequency. Two examples of the coupled mechanical–electrical types are presented. Specifically, the first configuration (denoted by coupled_1) has $R = 5000\ \Omega$ and $L = 1$ H, while the second configuration (denoted by coupled_2) has $R = 2500\ \Omega$ and $L = 0.5$ H. Obviously, there is only one pole in the amplitude, which corresponds to the resonant frequency 1.014 kHz, in the traditional mechanical impedance, as shown in Fig. 2(a). On the other hand, the addition of the electrical impedance brings about two more poles in each of the two configurations. Furthermore, the phase of the mechanical–electrical impedance becomes more complicated than that of the traditional mechanical impedance as plotted in Fig. 2(b).

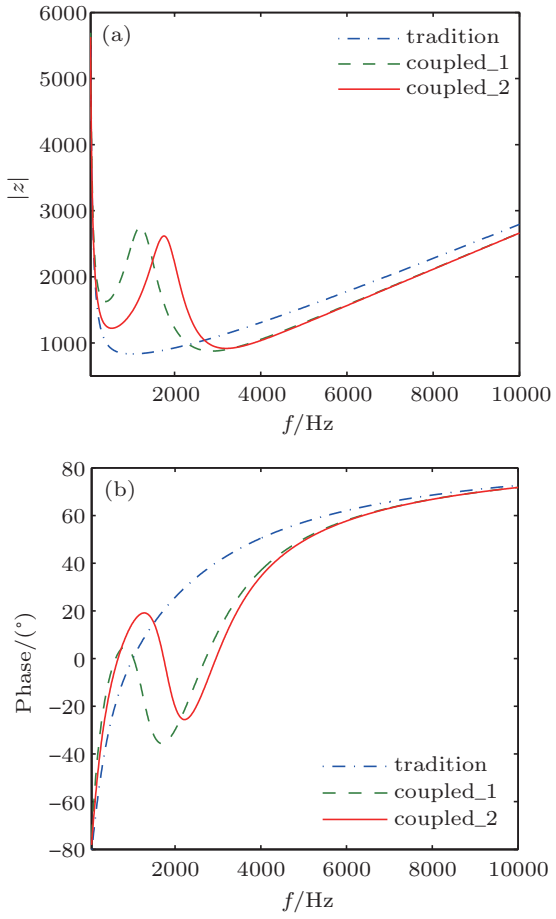


Fig. 2. (color online) (a) The amplitude and (b) the phase of the traditional mechanical impedance and two configurations of mechanical–electrical impedances.

Figure 3 plots the attenuation coefficients (defined by $A = |8.686 k_0 K_I|$, with K_I being the imaginary component of the wavenumber) of the first acoustic mode propagating in the downstream and the upstream directions under the influence of the acoustic impedance. It should be noticed that the features of high-order acoustic modes are not addressed, while such work can be easily implemented according to Eq. (8).

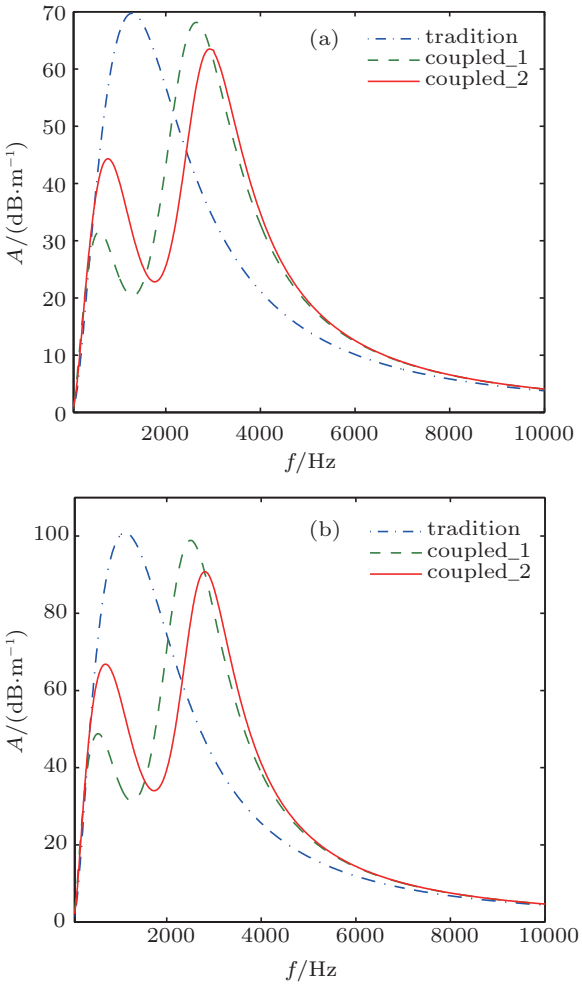


Fig. 3. (color online) The attenuation coefficients of the first acoustic mode propagating in (a) the downstream and (b) the upstream directions.

In the case of the traditional configuration with only the mechanical impedance, the attenuation coefficient reaches the maximum 69.7217 dB/m at 1.29 kHz in the downstream propagation and 100.8838 dB/m at 1.12 kHz in the upstream propagation. It can be learned that the acoustic frequency corresponding to the largest attenuation coefficient of the acoustic wave propagating downstream or upstream is not consistent with the resonant frequency 1.014 kHz of the mechanical impedance. Such inconsistency outlines the importance of the convection effect of fluid flow on the wave propagation. Generally, the flow convection contributes to larger attenuation coefficient in the upstream propagation compared with that in the downstream propagation. Furthermore, the flow-induced vortex shedding at the fluid–solid interface alters the process of the acoustic impedance of the pipeline wall, leading to different attenuation coefficients among upstream, stationary, and downstream conditions.

On the other hand, due to the electrical circuit, three poles (Fig. 3(a)) exist, which correspond to the three poles of the acoustic impedance (Fig. 2(a)). Compared with the traditional mechanical impedance where only one pole exists in the attenuation coefficient, it can be found that the performance of

wave attenuation can be significantly altered by changing the electrical component of the coupled impedance (see Figs. 2 and 3). Take note that the attenuation coefficients of the mechanical and the mechanical–electrical configurations become nearly the same as the acoustic frequency goes up, even when the difference of the amplitude of the acoustic impedance is significant. A possible explanation may be that the phases of the acoustic impedance in the two configurations turn out to be nearly identical when the acoustic frequency is high. It should be inferred that with the increase of the acoustic frequency, the amplitudes and the phases of the traditional mechanical and the coupled mechanical–electrical configurations may become identical, which leads to the same attenuation coefficients among the three examples, as shown in Fig. 3. However, by changing the electrical circuit loop, the attenuation coefficient in the mechanical–electrical configuration can be easily altered, which is demonstrated in the following two figures.

Specifically, figure 4 demonstrates the impedance and the attenuation coefficient of the mechanical–electrical configuration in the downstream and the upstream propagations as functions of the loaded inductor. The acoustic frequency is assumed as $f = 3$ kHz and the loaded resistor is $R = 5000\,\Omega$. Meanwhile, figure 5 illustrates the effect of the resistor on the impedance and the attenuation coefficient of the mechanical–electrical configuration. The acoustic frequency is assumed as $f = 3$ kHz and the loaded resistor is $L = 1$ H.

It can be found from Fig. 4 that the frequency corresponding to the maximum acoustic attenuation is not the pole of either the amplitude or the phase of the acoustic impedance. Such phenomenon can also be seen in Fig. 5. While a pole of the phase exists, there is no pole in the attenuation coefficient whenever the acoustic wave propagates downstream or upstream. There is no simple relationship between the attenuation coefficient and the acoustic impedance. Roughly speaking, the influence of the impedance phase on the attenuation coefficient is more significant than that of the impedance amplitude. From Figs. 4 and 5, one can infer that the alteration of the electrical loop through the inductor (Fig. 4) and the resistor (Fig. 5) can change the propagation attenuation of the acoustic wave in the downstream and upstream directions.

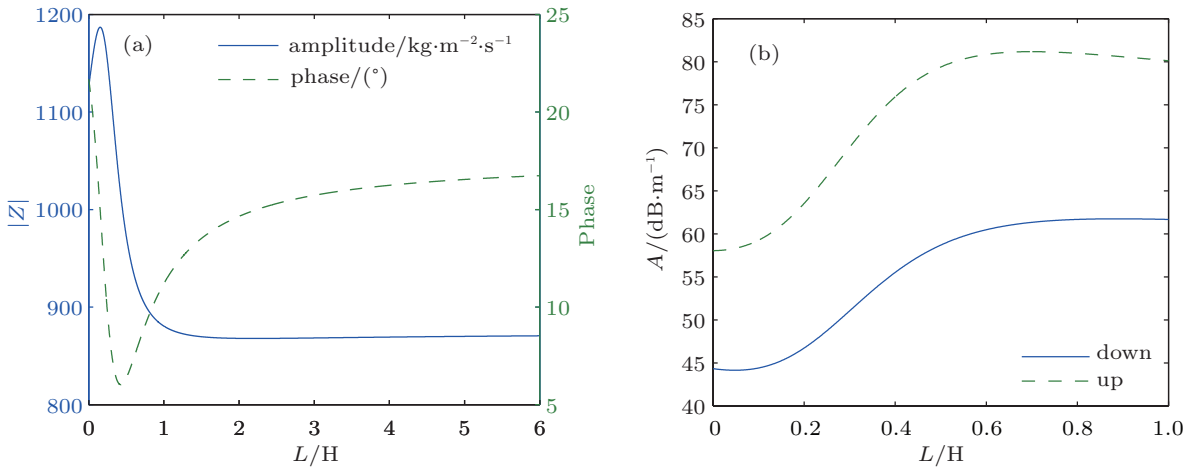


Fig. 4. (color online) The effect of the inductor on (a) the impedance and (b) the attenuation coefficient in downstream and upstream propagations.

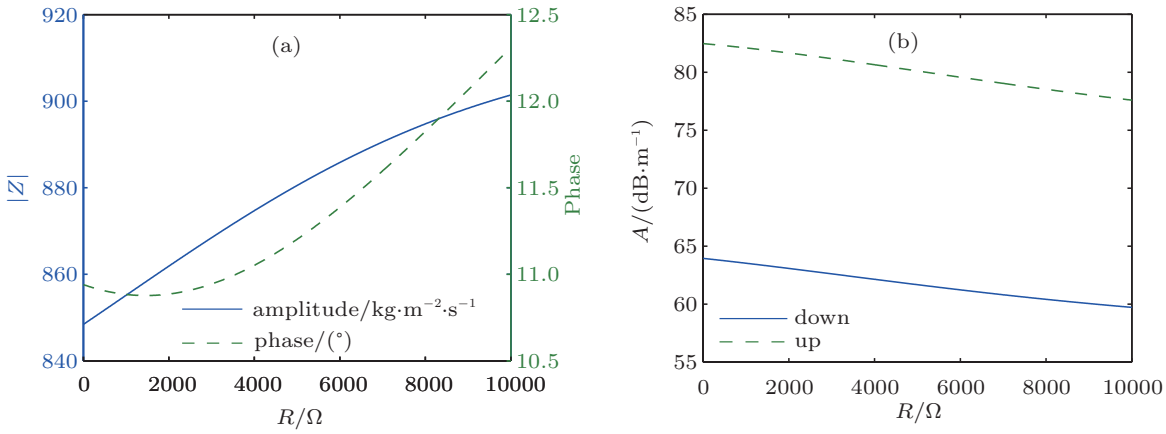


Fig. 5. (color online) The effect of the resistor on (a) the impedance and (b) the attenuation coefficient in downstream and upstream propagations.

4. Conclusion

We investigate coupled mechanical–electrical impedance configurations for aeroacoustic damping in a circular pipeline with a uniform flow. Our numerical study shows that the attenuation coefficient is dependent coherently on the amplitude and the phase of the acoustic impedance. While changing the two features independently may be difficult in the configuration of a mechanical resonator, the features can be easily adjusted through the electrical circuit loop in the coupled mechanical–electrical impedance. Due to the development of the micro-electro-mechanical system[21] and material technologies,[23] the proposed mechanical–electrical impedance of noise reduction may be fabricated without many difficulties. Moreover, the effect of the flow profile plays an important role on the wave attenuation, which alters the effect of the acoustic impedance of the resonator.

References

[1] Astley R J and Gabard G 2011 *J. Sound Vib.* **330** 3785
[2] Peat K S 1994 *J. Sound Vib.* **175** 475
[3] Lawrie J B 2009 *Proc. R. Soc. Lond. A* **465** 2347
[4] Rienstra S W and Hirschberg A 2013 *Report No. IWDE* 92-06
[5] Liang P N and Scarton H A 1996 *J. Sound Vib.* **193** 1099
[6] Brambley E J and Peake N 2006 *Wave Motion* **43** 301
[7] Twiefel J and Westermann H 2013 *J. Intell. Mat. Syst. Str.*
[8] Zhang W Y, Li Y L, Chang X Y and Wang N 2013 *Chin. Phys. B* **22** 098401
[9] Li P 2009 *Chin. Phys. B* **18** 4769
[10] Fan K Q, Ming Z F, Xu C H and Chao F B 2013 *Chin. Phys. B* **22** 104502
[11] Renno J, Daqaq M F and Inman D J 2009 *J. Sound Vib.* **320** 386
[12] Barrero-Gil A, Pindado S and Avila S 2012 *Appl. Math. Model.* **36** 3153
[13] Chen Q M and Wang Q M 2005 *Appl. Phys. Lett.* **86** 022904
[14] Wang X D, Song J H, Liu J and Wang Z L 2007 *Science* **316** 102
[15] Yang R, Qin Y, Da L M and Wang Z L 2008 *Nat. Nanotech.* **4** 34
[16] Liu S, Zhao S S, Sun B P and Zhang W M 2014 *Chin. Phys. B* **23** 094501
[17] Wang D A, Chiu C Y and Pham H T 2012 *Mechatronics* **22** 746
[18] Yu G L, Li Y X, Zeng Y Q, Li J, Zuo L, Li Q and Zhang H W 2013 *Chin. Phys. B* **22** 077504
[19] Fan K Q, Xu C H, Wang W D and Fang Y 2014 *Chin. Phys. B* **23** 084501
[20] Chen J, Zhu G, Yang W Q, Jing Q S, Bai P, Yang Y, Hou T C and Wang Z L 2013 *Adv. Mater.* **25** 6094
[21] Le C P and Halvorsen E 2012 *J. Micromech. Microeng.* **22** 074013
[22] Yang W Q, Chen J, Zhu G, Wen X N, Bai P, Su Y J, Lin Y and Wang Z L 2013 *Nano Research* **3** 211
[23] Chen J, Liu Y, Yang W Q, Su Y J and Wang Z L 2014 *ACS Nano* **8** 2649
[24] Lissek H, Boulandet R and Fleury R 2011 *J. Acoust. Soc. Am.* **129** 2968
[25] Chang D Q, Liu B L and Li X D 2010 *J. Acoust. Soc. Am.* **128** 623
[26] Betgen B and Galland M A 2011 *Mech. Syst. Sign. Proc.* **25** 1715
[27] Liu F, Horowitz S, Nishid T, Cattafesta L and Sheplakb M 2007 *J. Acoust. Soc. Am.* **122** 291
[28] Brambley E J 2011 *AIAA J.* **49** 1272
[29] Knutsson M and Abom M 2010 *J. Sound Vib.* **329** 4719
[30] Brambley E J, Davis A M J and Peake N 2012 *J. Fluid Mech.* **690** 399
[31] Richter C 2009 *Liner Impedance Modeling in the Time Domain with Flow* (Doctor dissertation) (Berlin: Berlin University of Technology)
[32] Alonso J S and Burdisso R A 2007 *AIAA J.* **45** 2677
[33] Brambley E J 2009 *J. Sound Vib.* **322** 1026
[34] Rienstra S W and Darau M 2011 *J. Fluid Mech.* **671** 559